Science of the Total Environment 859 (2023) 160249

Contents lists available at ScienceDirect

Science of the Total Environment

journal homepage: www.elsevier.com/locate/scitotenv

COVID-19 pandemic underscores role of green space in urban carbon dynamics

K. Hwang [a,*], S.A. Papuga [a,b]

[a] Department of Environmental Science and Geology, Wayne State University, Detroit, MI, United States of America
[b] Department of Hydrology and Atmospheric Sciences, University of Arizona, Tucson, AZ, United States of America

HIGHLIGHTS

- Reduced traffic during COVID-19 lowered CO_2 concentrations in Detroit.
- Urban vegetation shows greater carbon mitigation potential than traffic reductions.
- Planting trees may be effective for meeting carbon neutrality goals in urban areas.

GRAPHICAL ABSTRACT

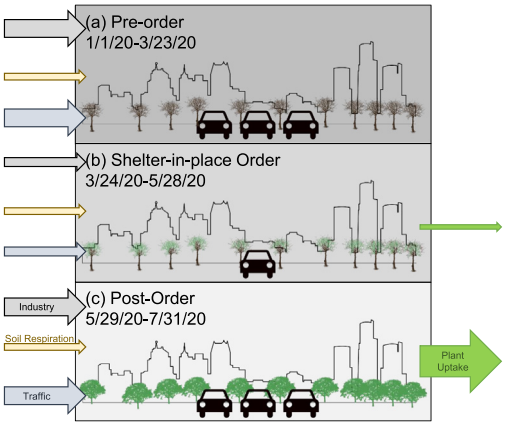

ARTICLE INFO

Editor: Kuishuang Feng

Keywords:
Vegetation
Shrinking city
Eddy covariance
Net ecosystem exchange
Carbon dioxide
Carbon emissions

ABSTRACT

For Detroit Michigan the arrival of COVID-19 led to intensive measures to prevent further spread of the virus resulting in consequent changes in traffic and energy use. We take advantage of these different emission scenarios to explore CO_2 dynamics in a postindustrial city with a declining population and increasing green space. We present atmospheric CO_2 concentration and net urban ecosystem exchange of CO_2 (*NUE*) from a typical eddy covariance system and canopy greenness from a field camera on the Wayne State University campus in midtown Detroit. We categorized our study period (January 18, 2020–July 31, 2020) into three subperiods associated with the state-wide shelter-in-place order. Our results support that the city was a net carbon source throughout the period, particularly during the shelter-in-place period, although reduced traffic lowered CO_2 concentrations and *NUE*. However, during the post-order period when traffic was highest, atmospheric CO_2 concentrations and *NUE* were lowest, suggesting that the greening of urban vegetation may have greater carbon mitigation potential than lowering anthropogenic carbon emissions through traffic reductions.

1. Introduction

The COVID-19 pandemic led to an abrupt global suspension of or reduction in many anthropogenic activities including industrial and commercial energy use and vehicular traffic worldwide. Researchers have taken advantage of this period to innovatively look at greenhouse gas emission scenarios in the context of climate change that otherwise has not been possible

* Corresponding author at: Institute of Arctic and Alpine Research, University of Colorado Boulder, Boulder, CO, United States of America.
E-mail address: kyotaek.hwang@colorado.edu (K. Hwang).

http://dx.doi.org/10.1016/j.scitotenv.2022.160249
Received 20 July 2022; Received in revised form 9 November 2022; Accepted 14 November 2022
Available online 17 November 2022

(Andreoni, 2021; Grivas et al., 2020; Lovenduski et al., 2021; Tian et al., 2021). From a global perspective, by assuming that emissions reductions scaled according to lockdown intensity, research suggests that mandated COVID-related confinements worldwide resulted in substantial temporary reductions in CO_2 emissions, ranging from about 9 to 17% lower when compared to the previous year (Le Quéré et al., 2020; Liu et al., 2020; Nicolini et al., 2022). For individual cities, research supports that these mobility restrictions could result in even larger emissions reductions (Turner et al., 2020; Velasco, 2021). Overall, these studies point toward the potential of reduction in traffic emissions as an effective strategy in mitigating climate change (Liu et al., 2020; Nicolini et al., 2022).

Notably, the recent CO_2 COVID-19 studies have tended to be focused on emissions, with less emphasis on uptake. The urban CO_2 budget can be simply expressed as:

$$NUE = C + R - P \quad (1)$$

Generally speaking, the net carbon dioxide exchange between the land surface and the atmosphere in urban settings (*NUE*) does tend to be dominated by fossil fuel combustion (*C*) from vehicles, industry, and individual households rather than the biological processes of photosynthesis (*P*) and respiration (*R*) (Crawford and Christen, 2015; Grimmond et al., 2002). Therefore, the focus on emissions is logical. However, some cities have extensive green spaces that have the potential to result in substantial carbon uptake through photosynthesis (Hardiman et al., 2017; Nordbo et al., 2012).

For instance, recent attention has been given to the phenomenon of urban shrinkage - substantial and long-term declines in population and economic activity that nearly 20% of cities worldwide have been experiencing (Beauregard, 2009; Blanco et al., 2009; Haase et al., 2013; Herrmann et al., 2016). These shrinking cities are now experiencing land use and land cover consequences of population decline (Beauregard, 2009; Herrmann et al., 2016). These consequences can include a substantially altered landscape newly covered with derelict vacant lots and brownfields (Haase et al., 2014; Kim, 2016; Schilling and Logan, 2008). With pressure to recover from this blight, shrinking cities are actively working to repurpose these spaces for their potential to contribute to the collective urban "green space" and the services it provides (Haase et al., 2014; Kim, 2016; Meerow and Newell, 2017). Particularly relevant is that greening a city's vacant lots has been shown to have the potential to offset direct carbon emissions (Vaccari et al., 2013) and CO_2 concentrations (Ng et al., 2015) by carbon sequestration. In sum, the urban shrinkage phenomenon is emerging as a new challenge (Haase et al., 2013; Herrmann et al., 2016), with the potential to have important consequences for global carbon cycling moving forward.

Detroit, Michigan is an example of a postindustrial city that has experienced a dramatic decrease in its population and economic base with expanding blight since the 1950s due to the declining motor industry similar to other Rustbelt cities (Berglund, 2020). This has resulted in over 100,000 vacant lots left abandoned and unmanaged (Herrmann et al., 2017). Like other cities across the globe, immediately after Michigan's first case was reported in the Detroit area on March 10, 2020, a state of emergency was declared. Aligned with state-wide progress of the COVID-19 pandemic, the State of Michigan announced the official shelter-in-place order as a lockdown strategy effective on March 24, 2020 for regulating the spread of the disease by minimizing face-to-face contact. In compliance with the executive order, all non-essential business services and operations were discontinued. As reported daily cases decreased and finally became steady, the state government finally lifted its order on June 1, 2020 following another executive order that eased non-essential activities from May 29, 2020.

Consistent with the recent COVID-19 pandemic-based global emissions studies (Le Quéré et al., 2020; Liu et al., 2020), we hypothesized that both atmospheric CO_2 concentration and net ecosystem exchange of CO_2 in urban Detroit (*NUE*) would be significantly lower during the shelter-in-place period than during pre- and post-order periods. We expected these reductions to occur mainly as a result of changes in traffic patterns and industrial activity within the City of Detroit. We further expected that reductions in emissions associated with the temporary changes would overshadow any uptake effect from the urban green spaces.

2. Materials and methods

2.1. Site description

Our study takes place in the City of Detroit, located in southeast Michigan, just across the Detroit River from Windsor, Ontario, Canada (Fig. 1). Detroit has a humid temperate climate as defined by Koppen-Geiger climate class Dfa (Peel et al., 2007). Normal annual temperature and precipitation are 10.2°C and 796 mm, respectively (Herrmann et al., 2017). Green space in Detroit (approximately 43% of total city parcels) includes vacant lots, parks and recreational areas (Fig. 1a) with a growing season generally between April and October. The majority of annual CO_2 emissions in Detroit comprise energy use of buildings and facilities (e.g., electricity, natural gas, and fuel combustion) and road traffic, approximately 63% and 30%, respectively (Carlson et al., 2014).

Since August 2019, we have been operating a standard eddy covariance (EC) system (Aubinet et al., 2012) about 5 m above the rooftop of Wayne State University's 3 story (11 m) tall Physics Building in midtown Detroit (42.353961°N, 83.069512°W; 193 m above sea level) (Fig. 1b). Therefore, the presumed source area (Fig. 1) for this ~16 m tall EC system is mostly developed with a medium-high population density, multistory buildings (commercial and residential uses) and with high commuter traffic. Small parks and open green spaces are scattered throughout the area with small green infrastructure patches (Fig. 1b). While wind direction varies by the time of day and season, the majority of the prevailing wind derives approximately from the west (Fig. 2; i.e., 285°–295° clockwise from the north).

2.2. Data collection

We present data from January 1, 2020 to December 31, 2021. For the purposes of this study, we focus on three main time periods associated with state-wide executive orders given by the Governor of Michigan that restricted mobility in the City of Detroit at the onset of the COVID-19 pandemic. Ultimately, this results in re: a "pre-order" period (January 18 to March 23), a "shelter-in-place" period (March 24 to May 28) and a "post-order" period (May 29 to July 31). Note that while 2020 was the only year that the restrictions were actually in place, we use these periods as defined both in 2020 and 2021 to enable comparison between the two years.

2.2.1. Eddy covariance and micrometeorological measurements

With adherence to Ameriflux protocol and applying commonly used corrections through the free Campbell Scientific EasyFlux® DL Program, 30-minute averaged CO_2 fluxes are calculated using 10 Hz measurements from an integrated open-path analyzer and sonic anemometer (IRGASON®; Campbell Scientific Inc., Logan, UT) that is oriented in the direction of the prevailing wind. The instrument simultaneously measures absolute carbon dioxide and water vapor, air temperature, barometric pressure, three-dimensional wind speed, and sonic air temperature. These data are then stored in a Campbell Scientific CR6 datalogger. Given the uncertainty and lack of standards associated with the determination of friction velocity u_* in urban settings (Crawford et al., 2011), we choose to adopt a u_* threshold of 0.15 m s^{-1} that is consistent with other urban studies (Salgueiro et al., 2020; Vivoni et al., 2020). A u_* threshold of 0.15 m s^{-1} results in a filtering of ~5% of our observations, which is also consistent with other urban studies using EC systems (Menzer and McFadden, 2017; Salgueiro et al., 2020).

Consistent with previous studies (e.g., Kurc and Small, 2007), to calculate daily *NUE*, a half-hour average for each day is obtained, i.e., g CO_2 m^{-2} (half hour)$^{-1}$, from all "good" half-hour data. We multiplied this average by 48, i.e., the number of half hours in any given day, to obtain an estimate of *NUE* in units of g CO_2 m^{-2} d^{-1}. Positive values of *NUE* correspond to a net source of CO_2 over 24 h, and negative values of *NUE* correspond to a net sink of CO_2 over 24 h (Kurc and Small, 2007).

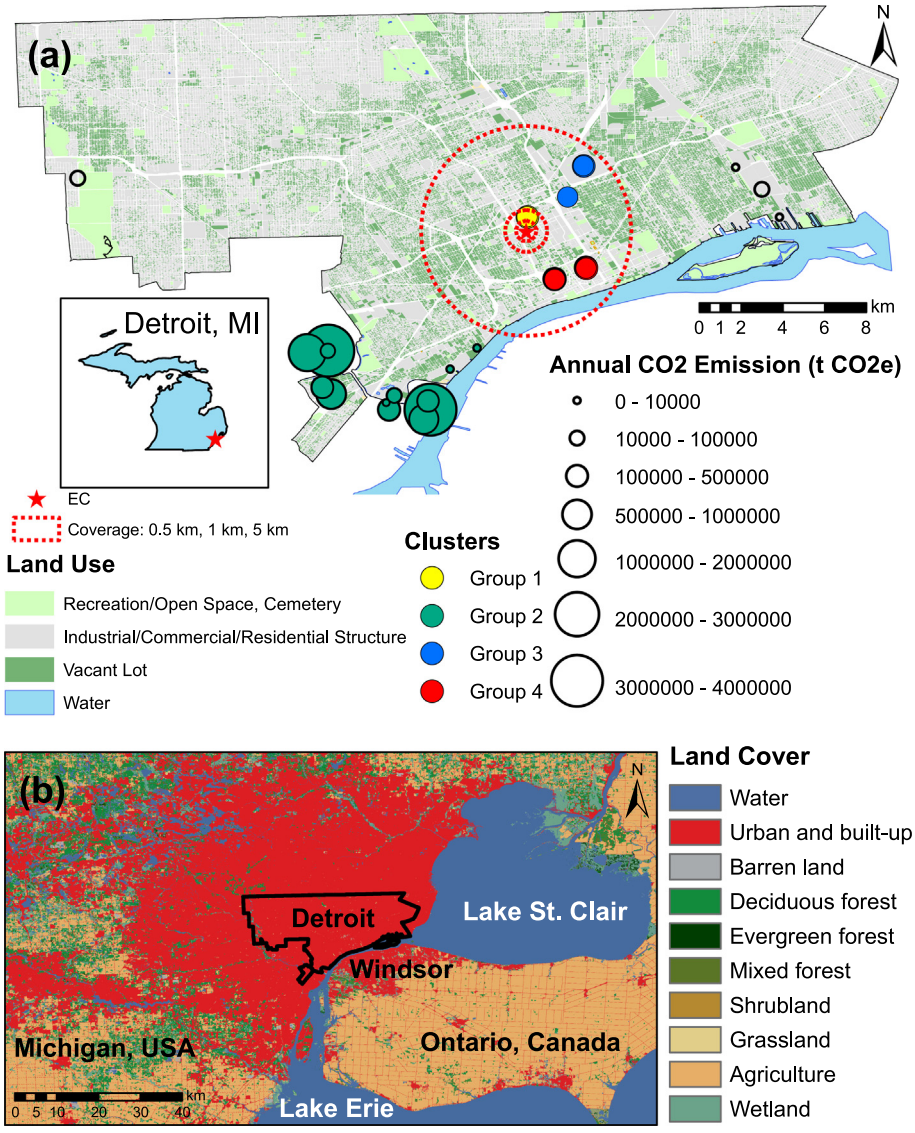

Fig. 1. The land use parcel map (a) specifically highlights the urban green spaces (vacant lots, recreation/open space/cemeteries) within the city limits of Detroit. Red concentric circles radiating out from the EC system (red star) represent 0.5 km, 1 km, and 5 km source areas. 2020 emission reports are also presented. The Landsat image-driven land use map (b) displays extensive urban sprawl in the Detroit metropolitan area that contributes to decentralized CO_2 emissions.

Additional micrometeorological measurements include air temperature and humidity (HMP155A, Vaisala, Helsinki, Finland), wind speed and direction (05103, RM Young Company, Traverse City, MI), and precipitation (CS700H, Campbell Scientific Inc., Logan, UT). Ethernet connection to university resources allows remote access to monitor instrumentation and collect data in real-time. Due to a power outage, measurements between February 26, 2020 and March 1, 2020, and November 24, 2021 and December 12, 2021 are missing.

2.2.2. Phenology camera and image analysis

A south-facing CCFC field camera (Campbell Scientific Inc., Logan, UT) is co-located with the EC system and captures hourly digital images of the downtown Detroit cityscape, including multiple tree canopy patches (Fig. 3). Because they tend to have optimal light conditions, we use the 2 pm (EST) images for estimating greenness. To estimate greenness, we identify nine static regions-of-interest (ROIs) within the 2 pm images that capture urban green space (Fig. 3). For each of the nine ROIs, we calculate a greenness index (I_g):

$$I_g = (green - red) + (green - blue) = (2 \times green) - (red + blue) \quad (1)$$

where red, green, and blue are the mean red, green, and blue intensities from the ROI, respectively (Kurc and Benton, 2010; Luketich et al., 2019; Richardson et al., 2007). To obtain a daily greenness index representing Detroit's urban green space, we average I_g values for the nine ROIs. This daily greenness index is normalized using min-max normalization for the entire study period.

2.2.3. Point emission sources

Twenty-two facilities in and around Detroit registered to the Environmental Protection Agency (EPA) Greenhouse Reporting Program (GHGRP) report annual total CO_2 emissions. We clustered these facilities into four groups based on their orientation from our EC system (Fig. 1b). The three groups within or near downtown (Group 1, 3, 4) are all domestic heating and energy suppliers. The southwest Downriver Group 2 facilities range from domestic heating to industrial emissions including power, iron, and steel production, municipal solid waste, hydrogen and oil production, and lime manufacturing. Based on EPA's most recent report from 2020, the largest emissions in this group were made by electricity generation (3,365,426 t CO2e yr^{-1}) and iron and steel production (1,741,148 t CO2e yr^{-1}).

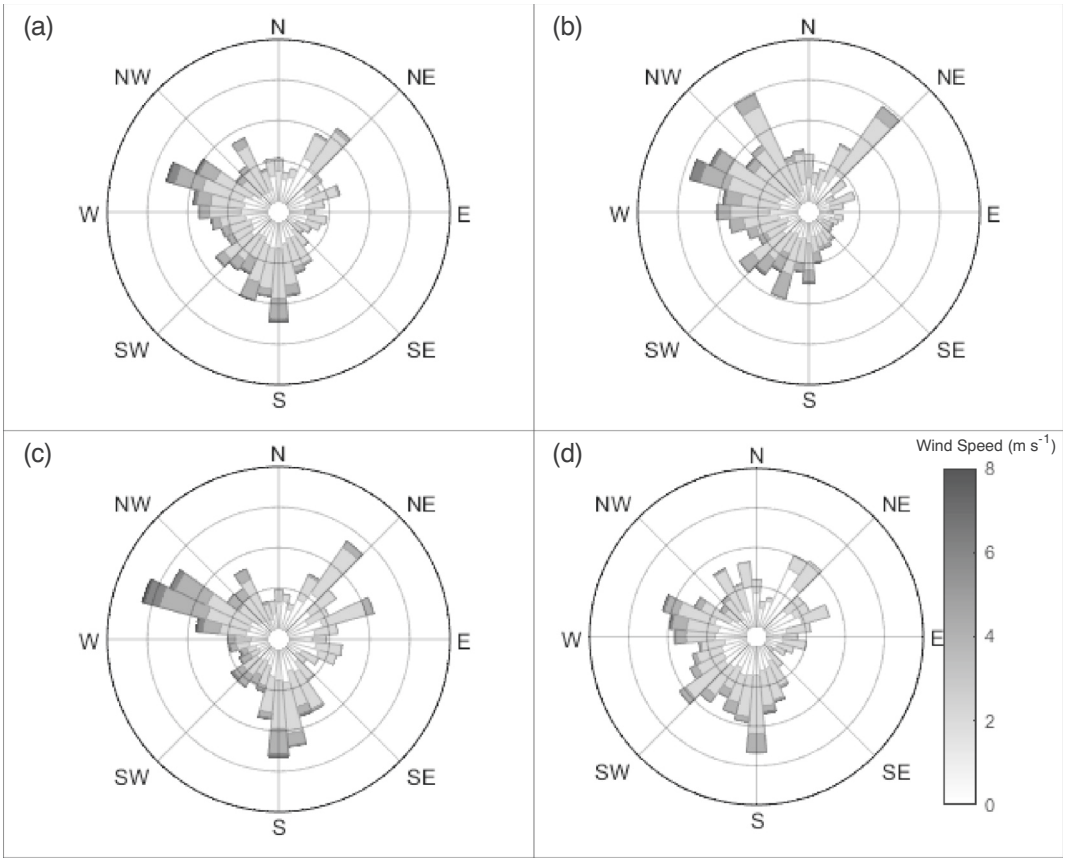

Fig. 2. Distribution of the wind speed and direction (a) over the whole study period, (b) in the pre-order periods, (c) in the shelter-in-place periods, and (d) post-order periods in 2020 and 2021.

2.2.4. Vehicular traffic

Vehicle Miles Traveled (VMT), a measure of daily road traffic as the total distance that all vehicles traveled in mega miles (Mmi), is estimated using the location records from smartphones and global positioning system (GPS) devices installed in motor vehicles associated with parcel and road network data by Streetlight Data Inc. (San Francisco, CA). Daily county-level VMT data over the US during the COVID-19 pandemic was obtained by individual contact to the provider. In this study, we used the Wayne County VMT data between January 1, 2020 and July 31, 2020 to represent Detroit road traffic.

We also used data from Mobility Trends Reports (MTR) to continue to observe traffic patterns throughout the growing season after VMT was no longer available. The MTR standardizes a daily volume of directions requests on the Apple Maps application on personal devices based on the

Fig. 3. Visual description of the field camera frame and ROIs. The sample image was acquired at 2 pm (EST) on June 14, 2020.

baseline volume on January 13, 2020 (Monday under regular traffic in Detroit). The dataset covers greater metropolitan areas over the world including Detroit during the global pandemic (January 13, 2020 to April 12, 2022 as of June 20, 2022). Global daily traffic data was open to the public for free by Apple Inc. (Cupertino, CA). We used the Detroit metropolitan MTR data from between January 13, 2020 and December 31, 2021.

Because the Detroit commutershed, Wayne County, and metropolitan Detroit do not perfectly overlap, the VMT and MTR product are imperfect proxies for vehicular emissions in our study; however VMT remains the method currently available to most cities (Hillman et al., 2011). We note the uncertainty associated with this approach and acknowledge it in the discussion.

3. Results

3.1. Precipitation and air temperature

Rainfall conditions were different in each of the categorized periods; pre-order totaled 41 mm, shelter-in-place totaled 158 mm, and post-order totaled 169 mm in year 2020 (Fig. 4a); pre-order totaled 12 mm, shelter-in-place totaled 138 mm, and post-order totaled 451 mm in year 2021 (Fig. 5a). Air temperature steadily increased throughout the study period, resulting in different temperature conditions in each of the categorized periods (Figs. 4b and 5b). In 2020, the minimum average air temperature −10.1°C occurred in the pre-order period on DOY 45 and the maximum average air temperature 28.7°C occurred in the post-order period on DOY 191 with a temperature range of 38.8°C. In 2021, the minimum average air temperature −10.6°C occurred in the pre-order period on DOY 38 and the maximum average air temperature 28.0°C occurred in the post-order period on DOY 186 for a temperature range of 38.6°C. Average air temperatures were 1.7°C, 10.6°C, and 23.7°C in year 2020 and 0.4°C, 12.9°C, and 22.8°C in year 2021 for the pre-order, shelter-in-place, and post-order periods respectively. Ultimately this resulted in cold, dry pre-order conditions and warm, wet post-order conditions.

3.2. Wind speed and wind direction

Wind speeds were higher and more variable in the pre-order and shelter-in-place periods than in the post-order period (Figs. 4b and 5b). In 2020, average wind speeds were 1.1 m s^{-1}, 0.8 m s^{-1}, and 1.0 m s^{-1} for the pre-order, shelter-in-place, and post-order periods respectively. In 2021, average wind speeds were 1.0 m s^{-1}, 1.4 m s^{-1}, and 1.3 m s^{-1} for

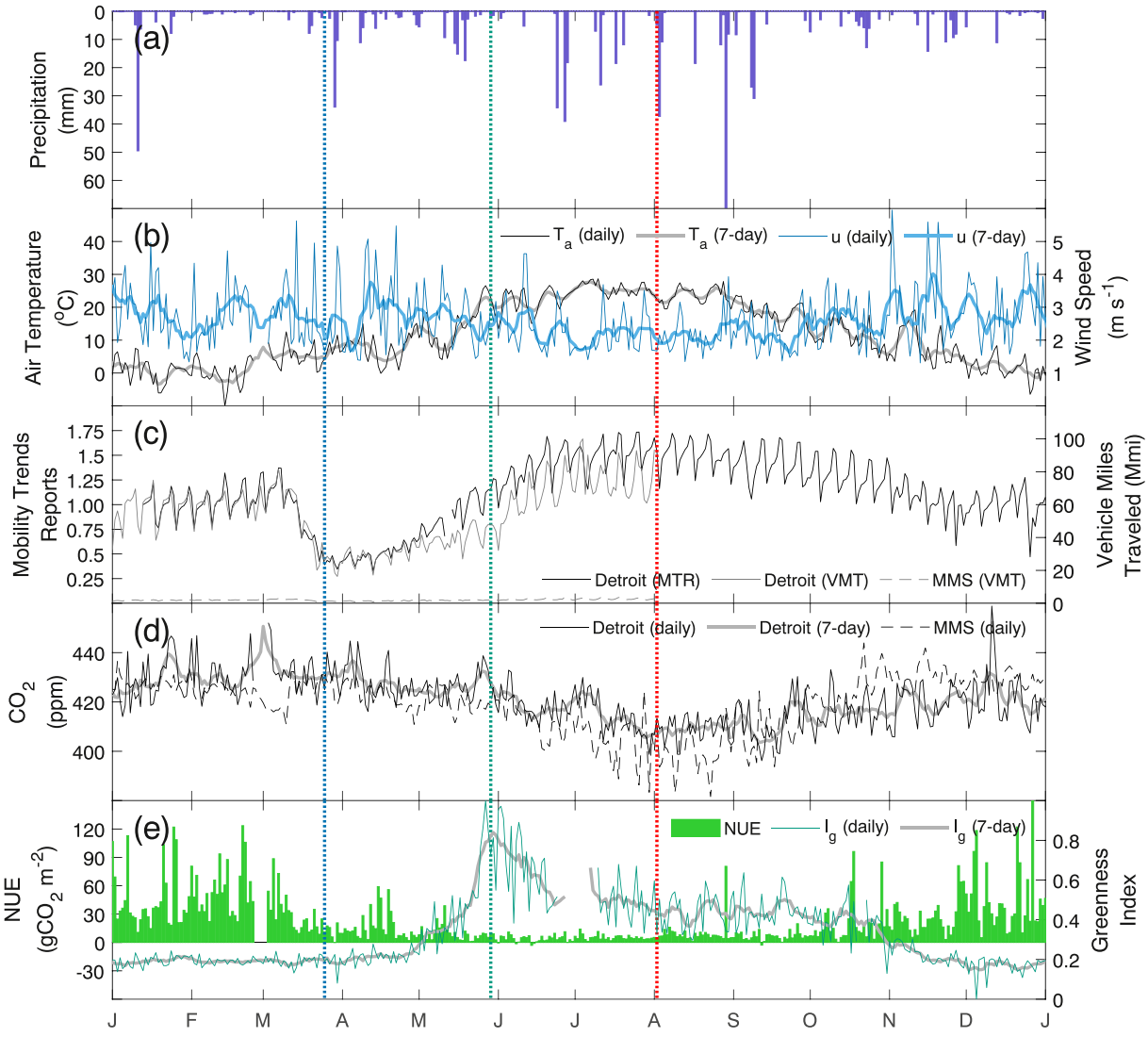

Fig. 4. Time series of year 2020 daily observations including the study periods where the vertical dotted blue, green, and red line indicate the end of the pre-order period, shelter-in-place period, and post-order period, respectively: (a) total precipitation, (b) daily and 7-day average air temperature (T_a) and wind speed (u), (c) city traffic data, (d) daily and 7-day average atmospheric CO_2 concentration, and (e) *NUE* and daily and 7-day normalized greenness index (I_g). CO_2 concentration and traffic of Morgan Monroe State Forest (US-MMS; data retrieved from the AmeriFlux website: https://ameriflux.lbl.gov/) are overlaid for comparison.

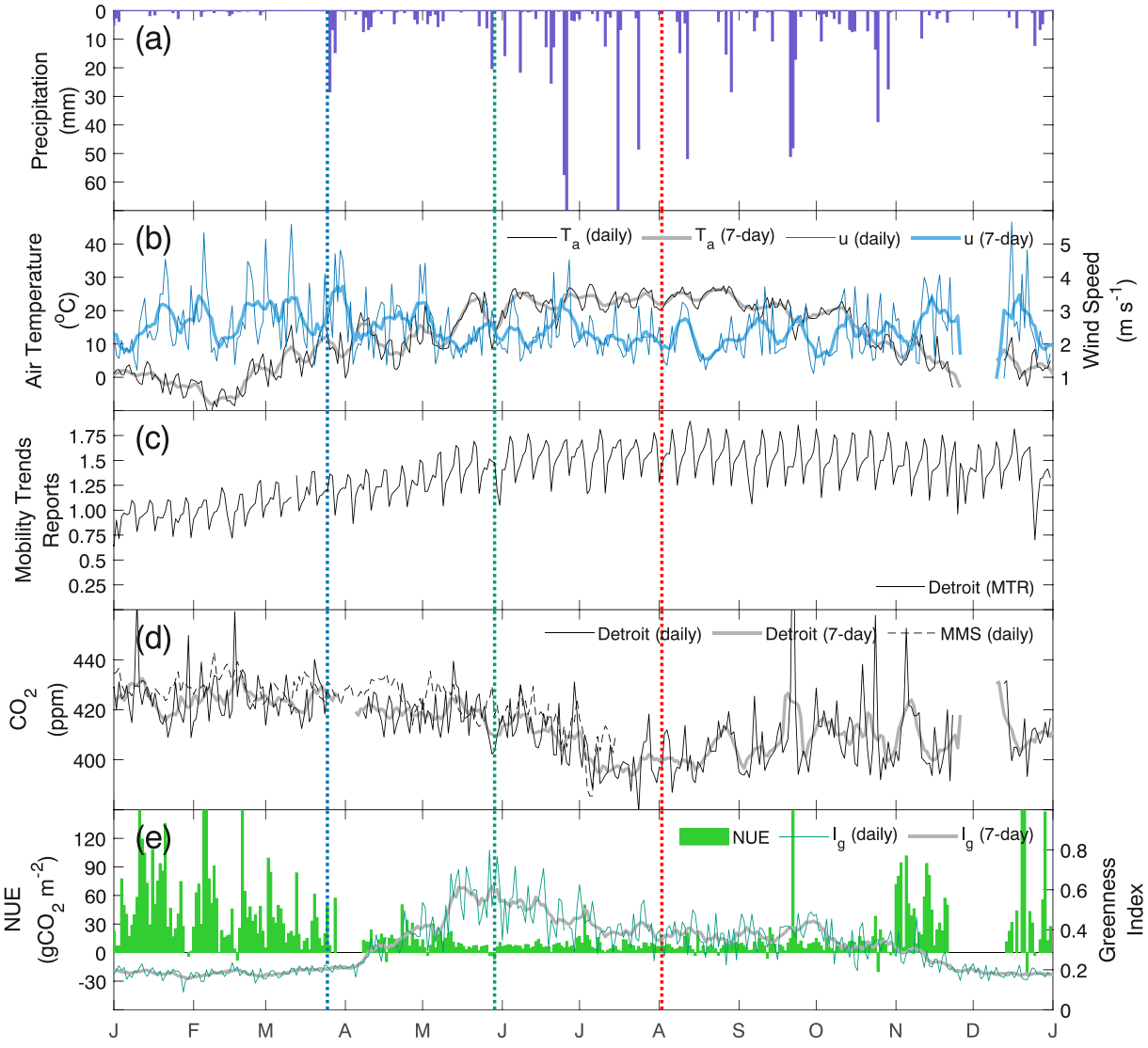

Fig. 5. Time series of year 2021 daily observations including the study periods where the vertical dotted blue, green, and red line indicate the end of the pre-order period, shelter-in-place period, and post-order period, respectively: (a) total precipitation, (b) daily and 7-day average air temperature (T_a) and wind speed (u), (c) city traffic data, (d) daily and 7-day average atmospheric CO_2 concentration, and (e) NUE and daily and 7-day normalized greenness index (I_g). CO_2 concentration of Morgan Monroe State Forest (US-MMS; data retrieved from the AmeriFlux website: https://ameriflux.lbl.gov/) are overlaid for comparison.

the pre-order, shelter-in-place, and post-order periods respectively. In 2020, average wind direction was 225°, 180°, and 211° for the pre-order, shelter-in-place, and post-order periods respectively. In 2021, average wind direction was 231°, 216°, and 214° for the pre-order, shelter-in-place, and post-order periods respectively.

3.3. Mobility trends

During the pre-order period, the traffic patterns were typical, averaging about 58 Mmi for VMT (Fig. 4c). Associated with the arrival of COVID-19 in Michigan on March 10, 2020, traffic began to quickly decrease during the pre-order period, ultimately reaching 57.6% of the pre-order mean traffic (i.e., 33 Mmi VMT) timed with the Governor's state-wide shelter-in-place order. Traffic recovery ramped up after Memorial Day (May 25, 2020) once the Governor began to lift travel restrictions, averaging 70 Mmi VMT and reaching a maximum of 100 Mmi VMT on July 3, 2020. For comparing our urban site with a natural setting that would not normally have much traffic, we pulled the data from the closest natural Ameriflux site, Morgan Monroe State Forest (US-MMS). As expected, at the US-MMS, VMT was 2 Mmi, 2 Mmi, and 3 Mmi for the pre-order, shelter-in-place, and post-order periods respectively (Fig. 4c).

Consistent with the VMT data, MTR shows substantial decrease associated with the shelter-in-place period in 2020; pre-order MTR was 0.99, shelter-in-place MTR was 0.67, and post-order MTR was 1.44 in year 2020 (Fig. 4c). By comparison, in year 2021, MTR was 1.05, 1.31, and 1.53 for the pre-order, shelter-in-place, and post-order periods respectively. Importantly, MTR was significantly different in the shelter-in-place period between 2020 and 2021 (p-value < 0.001).

3.4. CO_2 concentrations

Over the entire study period, daily CO_2 concentrations varied greatly, but generally decreased in both years between March and July. In 2020, CO_2 reached a high of 452 ppm on March 2 in the pre-order period and low of 399 ppm on July 29 in the post-order period (Fig. 4d). In 2021, CO_2 reached a high of 459 ppm on February 17 in the pre-order period and low of 379 ppm on July 24 in the post-order period (Fig. 5d). For 2020, in the pre-order period, daily CO_2 in Detroit ranged from 418 ppm

to 452 ppm with an average of 431 ppm (standard deviation = 8.0 ppm). For 2021, daily CO_2 in Detroit ranged from 409 ppm to 459 ppm with an average of 424 ppm (standard deviation = 9.3 ppm). During the shelter-in-place period, the range was lowered to between 416 and 441 ppm with an average of 426 ppm (standard deviation = 5.7 ppm) in year 2020 and to between 402 and 440 ppm with an average of 419 ppm (standard deviation = 7.4 ppm) in year 2021. For the post-order period the range was even lower, between 399 and 433 ppm, with an average of 416 ppm (standard deviation = 7.2 ppm) in year 2020 and between 379 and 431 ppm, with an average of 405 ppm (standard deviation = 11.1 ppm) in year 2021. For comparison, the US-MMS forest site had a range between 383–434 ppm (2020) and 385–443 ppm (2021) (Figs. 4d and 5d).

3.5. Net urban ecosystem exchange of CO_2

Overall, the City of Detroit was a source of CO_2 (*NUE* > 0) to the atmosphere, with the strength of that source varying throughout the study period (Figs. 4e and 5e). In both 2020 and 2021, *NUE* was highest in the pre-order period when traffic was high and the urban canopy was senesced (Figs. 4c, e and 5c, e). In 2020, as traffic was reduced associated with the Governor's order and as plants started to green up, *NUE* began to decrease and become close to zero (Fig. 4c, e). As traffic peaked up, but the urban canopy was still green, *NUE* was lowest. Specifically, average pre-order *NUE* was 46 $gCO_2\ m^{-2}$, average shelter-in-place *NUE* was 13 $gCO_2\ m^{-2}$, and average post-order *NUE* was 5 $gCO_2\ m^{-2}$ in year 2020. Despite no ordered traffic reductions in 2021, *NUE* still approached zero as the plants started to green up (Fig. 5c, e). Again, average pre-order *NUE* was 46 $gCO_2\ m^{-2}$, average shelter-in-place *NUE* was 13 $gCO_2\ m^{-2}$, and average post-order *NUE* was 8 $gCO_2\ m^{-2}$. By comparison, in 2020 the US-MMS forest site had an average 4 $gCO_2\ m^{-2}$ (pre-order *NUE*), 0 $gCO_2\ m^{-2}$ (shelter-in-place *NUE*), and $-22\ gCO_2\ m^{-2}$ (post-order *NUE*) and an average 3 $gCO_2\ m^{-2}$ (pre-order *NUE*), $-1\ gCO_2\ m^{-2}$ (shelter-in-place *NUE*), and $-20\ gCO_2\ m^{-2}$ (post-order *NUE*). The *NUE* difference between the pre-order and post-order in 2020 was $-41\ gCO_2\ m^{-2}$ in Detroit and -26 $gCO_2\ m^{-2}$ in US-MMS, suggesting that the productive urban green space could mitigate carbon emissions in combination with reduced energy consumption in summer.

3.6. Vegetation greenness

The normalized daily greenness index for both years of the study period exhibited a typical growing period trend (Figs. 4e and 5e). In both 2020 and 2021, greenness was low in the winter until budbreak in mid- to late-April when the urban canopy began to green up and then reached a peak in late May, sustaining greenness through the end of September. Greenness was lowest in the pre-order period with an average of 0.12 in 2020 and 0.11 in 2021. While peak greenness in both years was reached in late May during the shelter-in-place period (1.00 for 2020 and 0.78 for 2021), the average for the shelter-in-place period was 0.27 as compared 0.55 in the post-order period in 2020 and the average for the shelter-in-place period was 0.34 as compared 0.41 in the post-order period in 2021.

4. Discussion and conclusions

As expected, average daily CO_2 concentrations (Figs. 4d and 5d) and *NUE* differed between the study periods (Figs. 4e and 5e). On an annual scale, Detroit still acted as a net carbon source. Consistent with other studies (Bergeron and Strachan, 2011; Gratani and Varone, 2005; Helfter et al., 2011; Ward et al., 2013), peak CO_2 concentrations and *NUE* were in the pre-order periods which overlaps with wintertime conditions and energy demands. In 2020, CO_2 concentrations (Fig. 4d) and *NUE* (Fig. 4e) were lower in the shelter-in-place period than in the pre-order period. This is not surprising given Detroit road traffic decreased up to 30–50% of its typical rates during the shelter-in-place period (Fig. 4c) (Helfter et al., 2011). However, this was also the case for the shelter-in-place period in 2021 (Fig. 5d). This reduction in both years during the shelter-in-place period is not unexpected and is likely associated with a decline in domestic heating

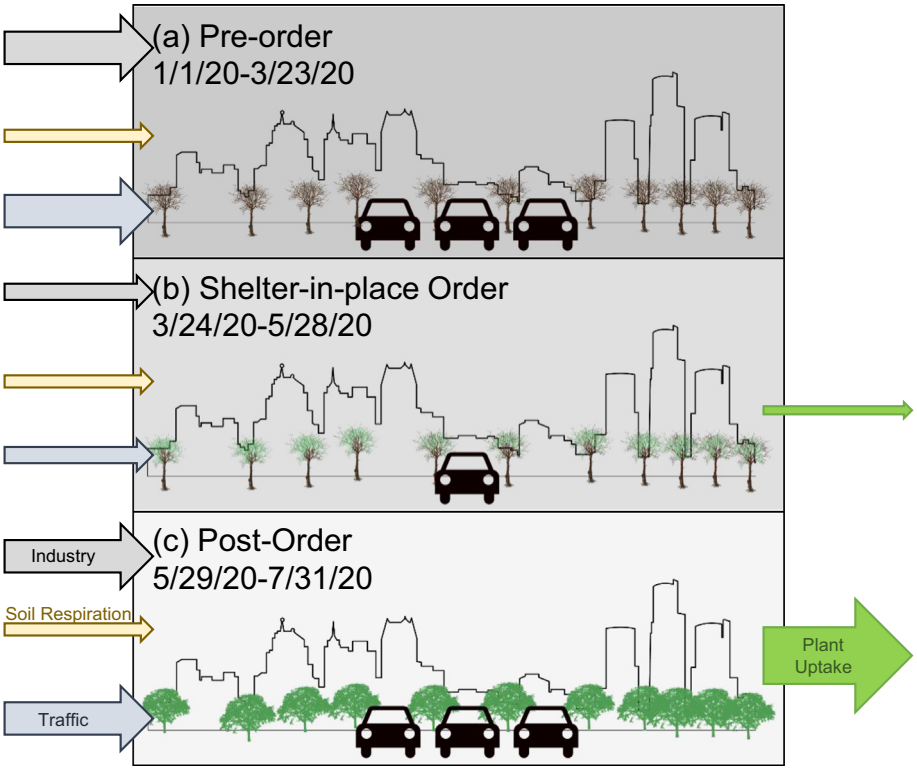

Fig. 6. Conceptual diagram of CO_2 concentration attributed to primary anthropogenic emissions and plant uptake for the (a) pre-order, (b) shelter-in-place, and (c) post-order periods. Darker background indicates greater CO_2 concentration. Widths of the arrows indicate the relative scale of incoming and outgoing CO_2 fluxes.

as space-heating CO_2 emissions tend to be negatively correlated with air temperature (Figs. 4b and 5b) (Crawford and Christen, 2015).

We expected *NUE* to be different in 2020 and 2021 during the shelter-in-place period because traffic was lower in 2020 than in 2021 due to the governor's order. However, *NUE* in 2020 and 2021 was not significantly different (p-value = 0.702) when MTR was (p-value < 0.001). What was further not expected was for the post-order period, when traffic exceeded pre-order levels in both 2020 and 2021, to have the lowest CO_2 concentrations and the lowest *NUE* (Figs. 4d–e and 5d–e). Some previous urban studies have also reported this unexpected pattern – heavier traffic in summer months without an associated increase in atmospheric CO_2 (Bergeron and Strachan, 2011; Crawford et al., 2011; Lia et al., 2020). Our data show that vegetation is overall greenest during the post-order period, suggesting that vegetation would have the most influence in this post-order period by sequestering carbon through its photosynthetic activity and storing it in biomass (Nowak and Crane, 2002; Ward et al., 2013). Notably, cities showing this unexpected pattern are either suburban or shrinking with a high percentage of green space (Bergeron and Strachan, 2011; Crawford et al., 2011); by parcel, green space is about 43% in Detroit (Fig. 1a). Under high CO_2 conditions from traffic emissions, this carbon uptake may even be accelerated during this period due to a potential fertilization effect (Lia et al., 2020; Reddy et al., 2010). This suggests that at least for cities with a declining population and an associated increasing amount of green space, the CO_2 uptake from vegetation could be substantial (Haase et al., 2014) and potentially outweigh the anthropogenic emissions during the growing season (Fig. 6).

Green space in urban ecosystems has the potential to reduce atmospheric CO_2 levels in multiple ways. During the growing season, plants directly sequester and accumulate CO_2 directly through photosynthesis. Urban vegetation provides shade and evaporative cooling in the summer months, decreasing building cooling demand (Akbari, 2002; Donovan and Butry, 2009; Jo, 2002). In the winter, the vegetation can reduce windspeed and provide insulation, also decreasing heating demand (Akbari, 2002; Jo, 2002). Therefore, urban vegetation indirectly lowers atmospheric CO_2 levels by reducing emissions associated with fossil fuel use (Jo, 2002; Nowak and Crane, 2002; Pataki et al., 2006). However, carbon stored in urban vegetation (Davies et al., 2011) can be lost to soils during litterfall, or removed and composted, in either case ultimately returned to the atmosphere via decomposition (Jo, 2002). Nevertheless, green space plays a key role in urban carbon dynamics and has enormous potential for offsetting urban CO_2 emissions, reducing atmospheric CO_2, and mitigating climate change (Akbari, 2002; Chen, 2020; Hong et al., 2019; Jo, 2002; Lia et al., 2020; Nowak, 1993; Wang and Shu, 2020; Zhao et al., 2010). The annual return on investment of planting and managing trees has been found to range from 37% to over 300% (McPherson et al., 2005). Therefore, urban green space planning and management has been lauded as a cost-effective strategy to mitigate climate change (Jo, 2002) when considering multiple ecosystem services.

CRediT authorship contribution statement

K. Hwang: Conceptualization, Data curation, Formal analysis, Writing – original draft, Writing – review & editing. **S.A. Papuga:** Conceptualization, Funding acquisition, Project administration, Writing – original draft, Writing – review & editing.

Data availability

Data will be made available on request.

Declaration of competing interest

The authors declare that they have no known competing financial interests or personal relationships that could have appeared to influence the work reported in this paper.

Acknowledgments

This research is supported by Wayne State University's College of Liberal Arts and Sciences and the Office for the Vice President for Research, NSF CNH award 1518376, NSF SRN award 1444758, and NSF EAR MCA award 2126206. We are also grateful for the help of field assistants Alex Eklund, David Reed, John Niedermiller, Elana Chan, and Cecily Valdez. Flux tower data are available in HydroShare: http://www.hydroshare.org/resource/2170c1bcedac4e1d817b256f1a539599. We acknowledge the following AmeriFlux site for its data records: US-MMS. In addition, funding for AmeriFlux data resources was provided by the U.S. Department of Energy's Office of Science. Apple Mobility Trends Reports data are available at https://covid19.apple.com/mobility. StreetLight Data Inc. supports vehicular Miles Traveled Monitor Metrics data for the purpose of nonprofit research in response to the COVID-19 pandemic. Synthesized nationwide point emission reports are publicly available through the Facility Level Information on GreenHouse gases Tool (FLIGHT): https://ghgdata.epa.gov/ghgp/main.do.

References

Akbari, H., 2002. Shade trees reduce building energy use and CO2 emissions from power plants. Environ. Pollut. 116, S119–S126.
Andreoni, V., 2021. Estimating the European CO2 emissions change due to COVID-19 restrictions. Sci. Total Environ. 769.
Aubinet, M., Vesala, T., Papale, D., 2012. Eddy Covariance: A Practical Guide to Measurement and Data Analysis. Springer, New York, NY.
Beauregard, R.A., 2009. Urban population loss in historical perspective: United States, 1820–2000. Environ.Plan.A-Econ.Space 41, 514–528.
Bergeron, O., Strachan, I.B., 2011. CO2 sources and sinks in urban and suburban areas of a northern mid-latitude city. Atmos. Environ. 45, 1564–1573.
Berglund, L., 2020. The shrinking city as a growth machine: Detroit's reinvention of growth through triage, foundation work and talent attraction. Int. J. Urban Reg. Res. 44, 219–247.
Blanco, H., Alberti, M., Olshansky, R., Chang, S., Wheeler, S.M., Randolph, J., et al., 2009. Shaken, shrinking, hot, impoverished and informal: emerging research agendas in planning. Prog. Plan. 72, 195–250.
Carlson, J., Cooper, J., Donahue, M., Neale, M., Ragland, A., 2014. City of Detroit Greenhouse Gas Inventory: An Analysis of Citywide and Municipal Emissions for 2011 and 2012. University of Michigan Center for Sustainable Systems, School of Natural Resources and Environment, Ann Arbor, Michigan.
Chen, Y.C., 2020. Evaluation of greenhouse gas emissions and energy recovery from planting street trees. Greenhouse Gases Sci. Technol. 10, 604–612.
Crawford, B., Christen, A., 2015. Spatial source attribution of measured urban eddy covariance CO2 fluxes. Theor. Appl. Climatol. 119, 733–755.
Crawford, B., Grimmond, C.S.B., Christen, A., 2011. Five years of carbon dioxide fluxes measurements in a highly vegetated suburban area. Atmos. Environ. 45, 896–905.
Davies, Z.G., Edmondson, J.L., Heinemeyer, A., Leake, J.R., Gaston, K.J., 2011. Mapping an urban ecosystem service: quantifying above-ground carbon storage at a city-wide scale. J. Appl. Ecol. 48, 1125–1134.
Donovan, G.H., Butry, D.T., 2009. The value of shade: estimating the effect of urban trees on summertime electricity use. Energy Build. 41, 662–668.
Gratani, L., Varone, L., 2005. Daily and seasonal variation of CO2 in the city of Rome in relationship with the traffic volume. Atmos. Environ. 39, 2619–2624.
Grimmond, C.S.B., King, T.S., Cropley, F.D., Nowak, D.J., Souch, C., 2002. Local-scale fluxes of carbon dioxide in urban environments: methodological challenges and results from Chicago. Environ. Pollut. 116, S243–S254.
Grivas, G., Athanasopoulou, E., Kakouri, A., Bailey, J., Liakakou, E., Stavroulas, I., et al., 2020. Integrating in situ measurements and city scale modelling to assess the COVID-19 lockdown effects on emissions and air quality in Athens, Greece. Atmosphere 11.
Haase, C., Dethlefsen, F., Ebert, M., Dahmke, A., 2013. Uncertainty in geochemical modelling of CO2 and calcite dissolution in NaCl solutions due to different modelling codes and thermodynamic databases. Appl. Geochem. 33, 306–317.
Haase, D., Haase, A., Rink, D., 2014. Conceptualizing the nexus between urban shrinkage and ecosystem services. Landsc. Urban Plan. 132, 159–169.
Hardiman, B.S., Wang, J.A., Hutyra, L.R., Gately, C.K., Getson, J.M., Friedl, M.A., 2017. Accounting for urban biogenic fluxes in regional carbon budgets. Sci. Total Environ. 592, 366–372.
Helfter, C., Famulari, D., Phillips, G.J., Barlow, J.F., Wood, C.R., Grimmond, C.S.B., et al., 2011. Controls of carbon dioxide concentrations and fluxes above central London. Atmos. Chem. Phys. 11, 1913–1928.
Herrmann, D.L., Schwarz, K., Shuster, W.D., Berland, A., Chaffin, B.C., Garmestani, A.S., et al., 2016. Ecology for the shrinking city. Bioscience 66, 965–973.
Herrmann, D.L., Shuster, W.D., Garmestani, A.S., 2017. Vacant urban lot soils and their potential to support ecosystem services. Plant Soil 413, 45–57.
Hillman, T., Janson, B., Ramaswami, A., 2011. Spatial allocation of transportation greenhouse gas emissions at the city scale. J.Transp.Eng.-ASCE 137, 416–425.
Hong, J.W., Hong, J., Chun, J., Lee, Y.H., Chang, L.S., Lee, J.B., et al., 2019. Comparative assessment of net CO2 exchange across an urbanization gradient in Korea based on eddy covariance measurements. Carbon Balance Manag. 14, 18.

Jo, H.K., 2002. Impacts of urban greenspace on offsetting carbon emissions for middle Korea. J. Environ. Manag. 64, 115–126.
Kim, G., 2016. Assessing urban forest structure, ecosystem services, and economic benefits on vacant land. Sustainability 8.
Kurc, S.A., Benton, L.M., 2010. Digital image-derived greenness links deep soil moisture to carbon uptake in a creosotebush-dominated shrubland. J. Arid Environ. 74, 585–594.
Kurc, S.A., Small, E.E., 2007. Soil moisture variations and ecosystem-scale fluxes of water and carbon in semiarid grassland and shrubland. Water Resour. Res. 43.
Le Quéré, C., Jackson, R.B., Jones, M.W., Smith, A.J.P., Abernethy, S., Andrew, R.M., et al., 2020. Temporary reduction in daily global CO2 emissions during the COVID-19 forced confinement. Nat. Clim. Chang. 10, 647–653.
Lia, Y., Gao, J., Dong, S.C., Zheng, J., Jiac, X., 2020. Study of CO2 emissions from traffic and CO2 sequestration by vegetation based on Eddy covariance flux measurements in suburb of Beijing, China. Pol. J. Environ. Stud. 29, 727–738.
Liu, Z., Ciais, P., Deng, Z., Lei, R.X., Davis, S.J., Feng, S., et al., 2020. Near-real-time monitoring of global CO2 emissions reveals the effects of the COVID-19 pandemic. <sb:contribution><sb:title>Nat. </sb:title></sb:contribution><sb:host><sb:issue><sb:series><sb:title>Commun.</sb:title></sb:series></sb:issue></sb:host> 11.
Lovenduski, N.S., Swart, N.C., Sutton, A.J., Fyfe, J.C., McKinley, G.A., Sabine, C., et al., 2021. The ocean carbon response to COVID-related emissions reductions. Geophys. Res. Lett. 48.
Luketich, A.M., Papuga, S.A., Crimmins, M.A., 2019. Ecohydrology of urban trees under passive and active irrigation in a semiarid city. Plos One 14.
McPherson, G., Simpson, J.R., Peper, P.J., Maco, S.E., Xiao, Q.F., 2005. Municipal forest benefits and costs in five US cities. J. For. 103, 411–416.
Meerow, S., Newell, J.P., 2017. Spatial planning for multifunctional green infrastructure: growing resilience in Detroit. Landsc. Urban Plan. 159, 62–75.
Menzer, O., McFadden, J.P., 2017. Statistical partitioning of a three-year time series of direct urban net CO2 flux measurements into biogenic and anthropogenic components. Atmos. Environ. 170, 319–333.
Ng, B.J.L., Hutyra, L.R., Nguyen, H., Cobb, A.R., Kai, F.M., Harvey, C., et al., 2015. Carbon fluxes from an urban tropical grassland. Environ. Pollut. 203, 227–234.
Nicolini, G., Antoniella, G., Carotenuto, F., Christen, A., Ciais, P., Feigenwinter, C., et al., 2022. Direct observations of CO2 emission reductions due to COVID-19 lockdown across European urban districts. Sci. Total Environ. 830.
Nordbo, A., Jarvi, L., Haapanala, S., Wood, C.R., Vesala, T., 2012. Fraction of natural area as main predictor of net CO2 emissions from cities. Geophys. Res. Lett. 39, 5.
Nowak, D.J., 1993. Atmospheric carbon reduction by urban trees. J. Environ. Manag. 37, 207–217.
Nowak, D.J., Crane, D.E., 2002. Carbon storage and sequestration by urban trees in the USA. Environ. Pollut. 116, 381–389.
Pataki, D.E., Alig, R.J., Fung, A.S., Golubiewski, N.E., Kennedy, C.A., McPherson, E.G., et al., 2006. Urban ecosystems and the North American carbon cycle. Glob. Chang. Biol. 12, 2092–2102.
Peel, M.C., Finlayson, B.L., McMahon, T.A., 2007. Updated world map of the Koppen-Geiger climate classification. Hydrol. Earth Syst. Sci. 11, 1633–1644.
Reddy, A.R., Rasineni, G.K., Raghavendra, A.S., 2010. The impact of global elevated CO2 concentration on photosynthesis and plant productivity. Curr. Sci. 99, 46–57.
Richardson, A.D., Jenkins, J.P., Braswell, B.H., Hollinger, D.Y., Ollinger, S.V., Smith, M.L., 2007. Use of digital webcam images to track spring green-up in a deciduous broadleaf forest. Oecologia 152, 323–334.
Salgueiro, V., Cerqueira, M., Monteiro, A., Alves, C., Rafael, S., Borrego, C., et al., 2020. Annual and seasonal variability of greenhouse gases fluxes over coastal urban and suburban areas in Portugal: measurements and source partitioning. Atmos. Environ. 223.
Schilling, J., Logan, J., 2008. Greening the Rust Belt a green infrastructure model for right sizing America's shrinking cities. J. Am. Plan. Assoc. 74, 451–466.
Tian, X.L., An, C.J., Chen, Z.K., Tian, Z.Q., 2021. Assessing the impact of COVID-19 pandemic on urban transportation and air quality in Canada. Sci. Total Environ. 765.
Turner, A.J., Kim, J., Fitzmaurice, H., Newman, C., Worthington, K., Chan, K., et al., 2020. Observed impacts of COVID-19 on urban CO2 emissions. Geophys. Res. Lett. 47.
Vaccari, F.P., Gioli, B., Toscano, P., Perrone, C., 2013. Carbon dioxide balance assessment of the city of Florence (Italy), and implications for urban planning. Landsc. Urban Plan. 120, 138–146.
Velasco, E., 2021. Impact of Singapore's COVID-19 confinement on atmospheric CO2 fluxes at neighborhood scale. Urban Clim. 37.
Vivoni, E.R., Kindler, M., Wang, Z.C., Perez-Ruiz, E.R., 2020. Abiotic mechanisms drive enhanced evaporative losses under urban oasis conditions. Geophys. Res. Lett. 47.
Wang, W., Shu, J., 2020. Urban renewal can mitigate urban heat islands. Geophys. Res. Lett. 47.
Ward, H.C., Evans, J.G., Grimmond, C.S.B., 2013. Multi-season eddy covariance observations of energy, water and carbon fluxes over a suburban area in Swindon, UK. Atmos. Chem. Phys. 13, 4645–4666.
Zhao, M., Kong, Z.H., Escobedo, F.J., Gao, J., 2010. Impacts of urban forests on offsetting carbon emissions from industrial energy use in Hangzhou, China. J. Environ. Manag. 91, 807–813.